

Fabrication and performance of graphene nanoelectromechanical systems

Robert A. Barton

Department of Applied and Engineering Physics, Cornell University, 212 Clark Hall, Ithaca, New York 14853

Jeevak Parpia

Department of Physics, Cornell University, Clark Hall, Ithaca, New York 14853

Harold G. Craighead^{a)}

Department of Applied and Engineering Physics, Cornell University, 205 Clark Hall, Ithaca, New York 14853

(Received 16 February 2011; accepted 28 June 2011; published 9 September 2011)

As a result of the recent progress in fabricating large-area graphene sheets, graphene-based mechanical devices have become vastly easier to manufacture and now show even greater promise for a range of applications. This article reviews the progress of resonant graphene nanoelectromechanical systems and the possible applications of this technology to signal processing, sensing, and other areas. After discussing recent advances in fabrication and measurement techniques that make graphene resonators a viable technology, the article presents what is known about the performance of graphene mechanical systems. The authors also highlight unresolved questions, such as the source of the dissipation in graphene resonators, and discuss the progress made on these issues to date. The authors conclude with a discussion of important future directions for graphene research and the applications for which graphene nanomechanical devices may be well suited. © 2011 American Vacuum Society. [DOI: 10.1116/1.3623419]

I. INTRODUCTION

Graphene, a single layer of carbon atoms in a honeycomb lattice, is a material of both scientific interest and technological promise.^{1,2} It has remarkable electronic properties, including ultrahigh electron mobility³ and the fact that its electrons have zero effective mass, so that it offers a window into the physics of the Dirac equation.⁴ The combination of its electronic properties and its two-dimensional geometry make it useful for a number of technologies, including chemical sensors,⁵ flexible and transparent electrodes,⁶ and high-frequency analog transistors.^{7,8} In addition to its electrical properties, graphene has unique mechanical properties. It is the strongest material ever measured, with a breaking strain of nearly 25%, and it is among the stiffest known materials, with a Young's modulus of 1 TPa.⁹ Therefore, it has also been suggested for use in mechanical applications such as switches,¹⁰ membranes separating disparate environments,^{11–14} and supports for transmission electron microscopy.¹⁵

Among the devices for which graphene appears almost ideally suited are nanoelectromechanical systems (NEMS), mechanical devices that have at least one dimension smaller than 100 nm.¹⁶ These devices are sometimes further classified into resonant and quasistatic NEMS¹⁷; here, we will focus mostly on resonant NEMS. Since the small size of NEMS makes them extraordinarily sensitive detectors of mass, force, and displacement, the ultimate limit would be a

resonator one atom thick, but reducing most materials to such small dimensions generally affects mechanical stability and stiffness. Graphene, however, is simultaneously one atom thick and enormously strong and stiff. Additionally, its electrical conductivity enables integrated electrical transduction, and its planar geometry lends itself easily to standard lithographic processing. Graphene's suitability for mechanical resonance applications has already been demonstrated in many experiments.

This article highlights the remarkably rapid progress made in the field of graphene nanomechanics during the past several years, much of which has been enabled by advances in growth and fabrication methods. We focus on the challenges associated with building a new class of two-dimensional resonator from graphene and utilizing it for applications. We discuss the strides already taken toward this goal in fabrication, actuation, and detection of graphene NEMS, and we discuss progress in other important performance areas like resonant quality factor and frequency reproducibility. We also discuss applications for which graphene resonators have already been used, including simultaneous sensing of mass, stress, and charge. Furthermore, we address the relevance of NEMS fabrication techniques to mechanical graphene devices that do not utilize resonance, such as electron transparent membranes for SEM and TEM studies. We conclude by examining the fields in which graphene nanomechanics are likely to have a large impact and speculate about what we can expect from graphene mechanical technology in the next few years.

^{a)}Electronic mail: hgcl@cornell.edu

II. FABRICATION

The basic element of a flexural mechanical resonator is a section of material that is suspended and free to resonate. Therefore, this section will discuss the methods that have been devised thus far to produce suspended graphene sheets. There are a number of ways of producing suspended graphene membranes, many of them developed for mechanical resonance applications. First, we discuss the various means by which graphene itself can be fabricated; then, we discuss how suspended and electrically contacted devices can be made from graphene.

A. Graphene production

Since graphite is composed of many stacked layers of graphene, simply rubbing graphite against a solid surface produces graphene. However, many attempts to fabricate graphene by this method produced only multilayer graphene that was difficult to locate.^{18–22} The recent explosion of graphene research was enabled by the discovery that monolayer graphene is visible in an optical microscope if it has been isolated on a layer of oxide of precisely chosen thickness on a silicon wafer.^{1,23–25} The visibility of graphene under these conditions, which is due to optical interference, enabled rapid examination of large surface areas to determine where single layer graphene is produced by even a very low throughput method. Thus, rubbing thin flakes of graphite on top of SiO₂ on silicon, which yields few samples of single layer graphene in a wide assortment of multilayer stacks, became a viable method of producing graphene. This technique, called “mechanical exfoliation,” is shown in Fig. 1(a); the visibility of graphene on an appropriate thickness of SiO₂ is shown in Fig. 1(b). While optical interference allows single layers of graphite to be distinguished from multiple layers, it was soon discovered that the number of layers in a stack of graphene sheets could be determined from its Raman spectrum, which enabled more quantitative confirmation that a given sample was indeed monolayer graphene.^{26,27} Being able to optically identify potential single layer candidates and confirming their thickness with Raman spectroscopy enabled production of the first suspended graphene sheets via mechanical exfoliation, as we will discuss.

Mechanical exfoliation of graphene is still common practice today. However, locating graphene amid the assortment of thicker graphite produced by mechanical exfoliation is painstaking work, and the technique is not scalable. Fortunately, a number of other techniques are used to fabricate graphene in large areas. Epitaxial graphene growth, in which graphene is formed by sublimating silicon from silicon carbide, has been used to grow large-area graphene.^{28,29} Two-dimensional assemblies of reduced graphene oxides also have been heavily studied,^{30–32} and although they do not exhibit the electronic properties of graphene, they exhibit excellent mechanical properties³³ and may be well suited for NEMS.

Another approach is to grow graphene on metals by chemical vapor deposition (CVD). In early steps toward this method, graphene was synthesized on ruthenium³⁴ and iridium.³⁵ For device fabrication purposes, a major achievement was the

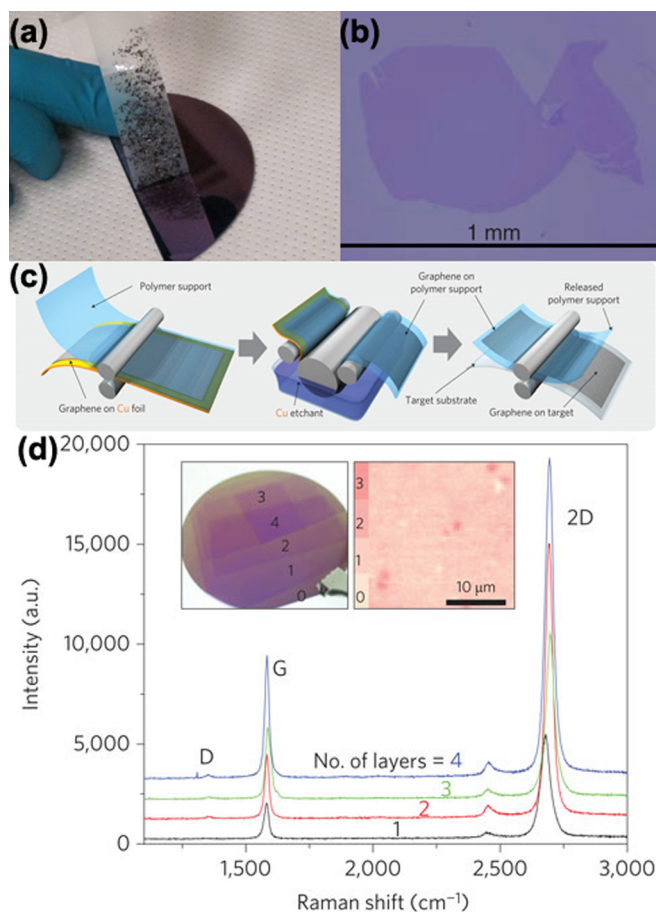


FIG. 1. (Color online) (a) Synthesis of graphene by mechanical exfoliation. Graphite is thinned by repeatedly peeling layers apart with scotch tape, then rubbed against a layer of oxide on a silicon wafer. (b) An exceptionally large graphene flake obtained by exfoliation. Reproduced from Ref. 2. (c) Schematic for producing large-area graphene from graphene grown on copper foil, adopted from Ref. 38. Graphene is produced on a roll of copper foil and attached to a polymer support using light pressure between two rollers. Using additional rollers, the copper is dissolved and the graphene is transferred to the final substrate. (d) The results of a similar process on a silicon wafer, together with an optical image showing more than 95% monolayer coverage. The graphene can be stacked to form several-layer-thick sheets, and Raman spectra for various graphene thicknesses are shown. Reproduced from Ref. 38.

growth of few-layer graphene on nickel, which allowed both large-area growth and isolation of the graphene from the metal.^{6,36} Unfortunately, graphene growth on nickel was characterized by regions with large numbers of layers. Soon thereafter, graphene growth by chemical vapor deposition on copper was found to produce up to 95% single layer graphene, with most of the rest bilayer graphene.³⁷ Since this discovery, much progress has been made in growing graphene by CVD on copper, including the production of graphene on rolls of copper³⁸ [(Figs. 1(c) and 1(d)] and the production of graphene from solid sources on copper using temperatures as low as 800 °C.³⁹ Recent studies of graphene produced by CVD on copper showed that it is polycrystalline^{40,41} and that its mechanical strength was weakened at its grain boundaries.⁴² However, slightly modified growth methods have been observed to produce graphene with much larger grain sizes.⁴³ It is suspected that further work on this growth method will yield graphene with fewer bilayer regions and larger grain sizes.

B. Fabrication of mechanical devices

The first suspended graphene sheets were produced using mechanical exfoliation, relying on the ability to identify graphene on an oxide surface.^{26,44,45} In one method,^{26,45} graphene sheets were produced by mechanical exfoliation on a standard SiO₂ surface and modified by electron-beam lithography and etching to produce suspended graphene sheets on a metallic scaffold for transmission electron microscopy. In another experiment,⁴⁴ mechanical exfoliation was used to fabricate graphene on top of predefined trenches in SiO₂, resulting in a doubly clamped beam that was confirmed to be monolayer graphene by Raman spectroscopy [Figs. 2(a) and 2(b)]. In both cases, only a small number of samples were produced. Nonetheless, the advent of suspended graphene proved very useful for the graphene community. Bolotin *et al.* showed that suspended graphene could be used to achieve ultrahigh electron mobility,³ making exfoliated suspended graphene instrumental in the recent observation of the fractional quantum Hall effect in graphene.^{46,47} It is also possible to produce enclosed volumes sealed by exfoliated

graphene,⁴⁸ as in Figs. 2(c) and 2(d), and to use lithography to produce arrays of graphene resonators of different lengths and shapes from exfoliated graphene, as shown in Figs. 2(e)–2(g).⁴⁹ Mechanical exfoliation is still used today to produce mechanical resonators⁵⁰ and other types of devices from graphene because it yields strips of very clean graphene without the need for lithography. Additionally, the continual refinement of the exfoliation technique has enabled the production of very large suspended graphene sheets with dimensions on the order of 50 μm .⁵¹ However, the technique is not scalable to producing large numbers of devices.

A more scalable means of graphene device production involves first growing a large-area sheet of graphene and subsequently processing it to create devices. In some cases, the graphene can be processed on the surface on which it was grown. For example, it is possible to grow graphene on top of copper and subsequently remove the copper, resulting in arrays of field effect transistors.⁵² Similarly, it is possible to fabricate suspended graphene for TEM studies by selectively etching copper from beneath graphene grown by CVD.⁵³ It is also possible to make nanomechanical resonators by, for

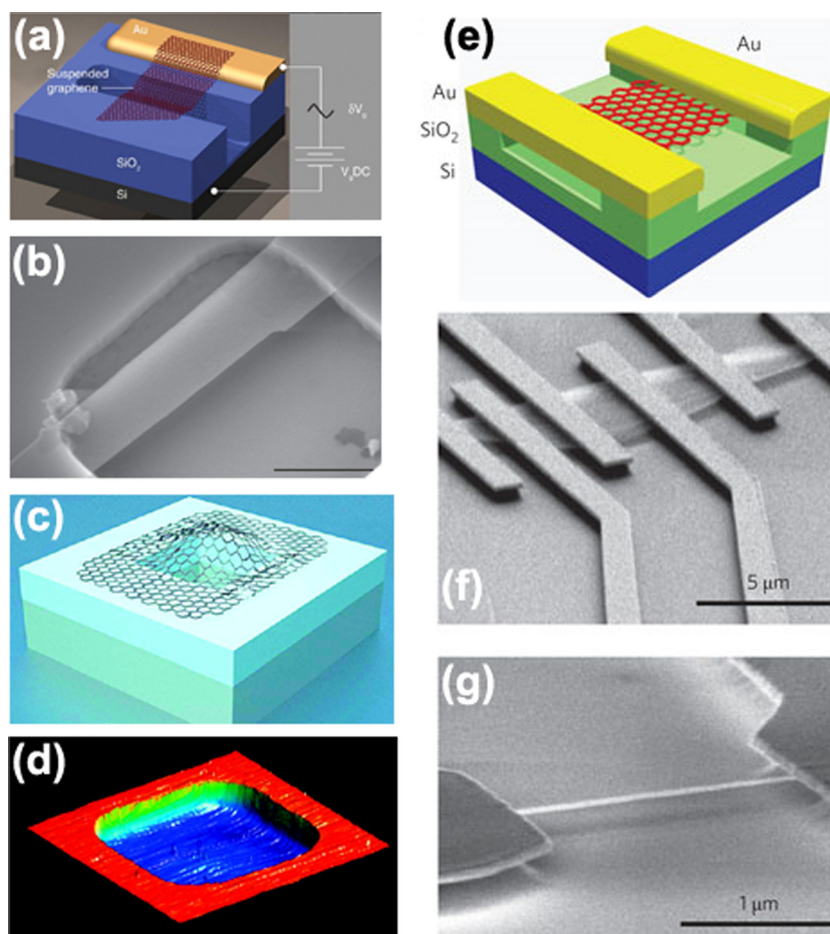


FIG. 2. (Color online) Graphene resonators made by mechanical exfoliation. (a), (b) Schematic and SEM image of a graphene resonator made by exfoliating graphene over a trench, reproduced from Ref. 44. (c), (d) Schematic and AFM image of a graphene resonator made by exfoliating graphene over a well. The graphene sheet (c) bulges upward in response to pressure, and (d) self-tensions by adhering to the sidewalls of the well when not acted on by other forces. Reproduced from Ref. 48. (e)–(g) Schematic and SEM images of graphene resonators fabricated by mechanical exfoliation followed by lithographic processing. Reproduced from Ref. 49.

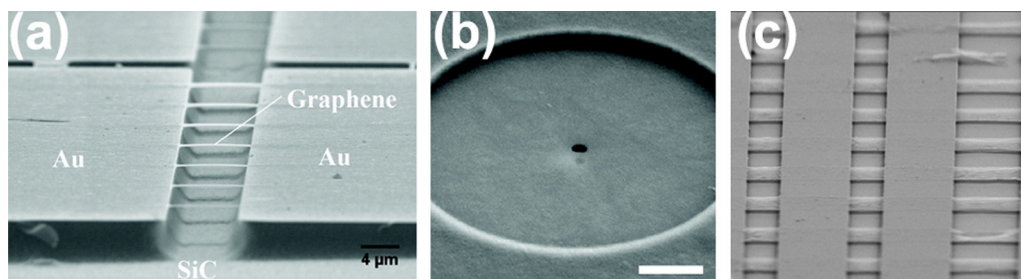


FIG. 3. (Color online) Graphene resonators made using large-area graphene. (a) Epitaxial graphene resonators fabricated by shaping the graphene on SiC and undercutting it using a wet etch (Ref. 54). (b) Resonators made of reduced graphene oxide. Scale bar, 1 μm (Ref. 56). (c) Arrays of doubly clamped beam resonators (2 and 5 μm in length) made from CVD graphene (Ref. 59).

example, etching silicon carbide from beneath graphene grown epitaxially on SiC [Fig. 3(a)].⁵⁴ However, the substrates on which graphene can be grown are not necessarily the ideal substrates for devices. For example, the nanomechanical devices fabricated in Ref. 54 were electrically shorted to their doped SiC substrate and could not be probed electronically. For this reason, we focus on what has been the primary approach to creating graphene mechanical devices thus far, which is growing graphene and subsequently transferring it to another surface for processing.

Transferring graphene after its growth is often necessary for a number of reasons. First, CVD growth from gaseous sources requires temperatures greater than 900 °C, which poses a challenge for semiconductor processing.³⁹ Second, the small-scale patterning required to make graphene devices is more easily done on standard silicon wafers than on the metal that facilitates graphene growth. Finally, it is often useful to isolate the graphene from the substrate on which it is grown, as in the case of the SiC-derived devices mentioned earlier. Currently, the most widely employed transfer method begins with graphene grown on copper, which we will discuss in detail here. However, transferring graphene produced by other methods, including mechanical exfoliation⁵⁵ and CVD on nickel,¹⁰ has been useful for many applications. It is also possible to make few-layer graphene resonators out of reduced graphene oxide transferred to a patterned substrate [see Fig. 3(b)].⁵⁶

The transfer of graphene from copper follows earlier procedures developed to transfer graphene from nickel.³⁶ Following growth of graphene on copper, the graphene is typically coated with a thin polymer layer such as PMMA (Ref. 37) or thermal release tape^{38,57} to maintain mechanical stability during transfer. Then, the copper is removed by etching with a chemical such as ferric chloride or ammonium persulfate. We note that ferric chloride has been observed to contaminate the surface of graphene with iron,^{40,53} which is problematic for some applications. Following the dissolution of copper, the graphene is rinsed in water and brought into contact with the final substrate. Finally, the support layer is removed to leave single layer graphene on an arbitrary surface. Typically, PMMA has been removed using acetone,⁵⁸ methylene chloride,⁵⁹ or thermal decomposition at 300 °C.⁶⁰

This transfer method is robust and can be used to make mechanical devices of many shapes and sizes. For example,

to make the electrically contacted, doubly clamped beam resonators described in Ref. 59, CVD-grown graphene was transferred to SiO₂, patterned using lithography and oxygen plasma, and contacted by evaporated electrodes. Then, a buffered oxide etch was used to remove the oxide from beneath the device, leaving it free to resonate. In another approach to making doubly clamped graphene beam resonators, graphene was patterned into strips while it was still on the copper using lithography and oxygen plasma. Then, the typical transfer process was used to place the strips on top of prefabricated trenches or electrodes. A similar approach was used to make mechanical switches out of graphene.¹⁰ Fabricating mechanical devices from graphene does not require shaping graphene lithographically. The drumhead resonators in Ref. 61 were fabricated by simply transferring graphene onto a circle defined in silicon nitride. Figures 3(b) and 3(c) show some of the devices that have been made using the transfer of large-area graphene.

III. PERFORMANCE, CHALLENGES, AND APPLICATIONS

Although graphene possesses many properties that seem to make it ideal for mechanical resonance applications, its promise must be validated by experiments. Here, we describe the challenges associated with making useful electromechanical resonators from graphene and describe the efforts designed to overcome these challenges.

A. Actuation and detection of mechanical motion

The performance of a nanomechanical resonator as, for example, a mass sensor is often limited by the readout technology.⁶² Hence, the transduction of graphene resonator motion is critical to the success of graphene NEMS. We briefly review the methods that have been developed to drive and detect the motion of graphene resonators.

The motion of the first graphene electromechanical resonators⁴⁴ was monitored via an optical interferometric effect.⁶³ Briefly, a laser impinges on the device perpendicular to the plane of the graphene sheet, reflecting from both the graphene and a silicon backplane beneath the device. The graphene and the reflective backplane form a Fabry–Perot interferometer that transduces device motion into variations in the reflected light intensity; these variations are

monitored by a fast photodiode connected to a spectrum analyzer. This technique has been used in several instances to measure the motion of graphene resonators,^{56,59,61} and it has the advantage of being able to transduce the motion of any suspended graphene sheet without requiring electrodes. Future work utilizing on-chip optical components may even enable portable optical readout. However, the method currently requires bulky optics and can cause issues with laser heating. Electrical readout was a logical next step to enable portable graphene nanoelectromechanical systems.

Electrical transduction was demonstrated in graphene⁴⁹ using a technique first developed to detect the motion of carbon nanotubes.⁶⁴ This technique overcomes the high-frequency impedance issues associated with monitoring electrical signals from nanomechanical resonators by using the resonator itself to mix down the signal to a lower frequency. The measurement is accomplished by suspending a graphene sheet above a backgate between two electrodes (source and drain). A dc voltage is applied to the gate in order to tension the device, while an oscillating gate voltage at frequency f is applied to the gate to drive resonator motion via capacitive attraction. A second rf voltage at frequency $f + \Delta f$ is applied to the source. Because the graphene conductance G changes with distance from the gate, G oscillates with frequency f on resonance, while the source–drain voltage V is oscillating with frequency $f + \Delta f$. The result is a mixed-down source–drain current $I = VG$ at Δf . For graphene, this technique gives ~ 60 dB dynamic range while allowing frequency tuning of $\sim 100\%$ via the backgate.⁴⁹ Variations on this method have been demonstrated to improve signal to noise even further.⁶⁵

The major drawback of the mixing technique is its speed.⁵⁰ Operating at the frequency Δf (typically ~ 1 kHz) significantly limits operation bandwidth and prevents rf applications of these oscillators that would require direct readout of frequency. To transduce the motion of NEMS at megahertz frequencies; however, one needs to increase the RC-limited cutoff frequency. In systems with a global backgate (often, the entire wafer acts as the gate), this cutoff frequency is set by unnecessary stray capacitance between the source and drain electrodes and the gate. Xu *et al.* eliminated this problem by employing a local backgate to reduce stray capacitance.⁵⁰ In this geometry, current across a source and drain was measured while a driving force was applied to the resonator by the local backgate. They found that the resonance could be observed through the change in current at the resonant frequency of the device due to the gate-tunable conductance of the graphene. At the expense of more stringent fabrication, this technique allowed them to acquire a given data set ~ 100 times faster than with the mixing technique, while maintaining comparable signal to noise.

It is worth noting that other drive mechanisms hold much promise for graphene NEMS. In particular, nonresonant oscillatory motion of very small, high-frequency resonators has been actuated and detected using scanning tunneling microscopy.⁶⁶ These devices have an estimated frequency of 400 GHz and could allow highly sensitive mass detection or exploration of quantum behavior in mechanical oscillators.

However, driving the resonant motion of these devices will be challenging.

Actuating motion of most graphene NEMS has proven simpler than detecting it. Both electrical and optical drive methods have been used to drive graphene over its full dynamic range; that is, from a minimum vibrational amplitude comparable to thermal fluctuations to a maximum vibrational amplitude characterized by the onset of Duffing nonlinearity.¹⁷ In most cases, electrical drive uses capacitive attraction to drive the motion of the resonator relative to a gate, as described earlier. The optical method utilizes a strobed laser whose light is partially absorbed by the graphene sheet, so that the sheet is periodically heated and cooled at the driving frequency; thermal expansion and contraction then convert these temperature changes into device motion.⁶⁷ Using the optical method, resonator motion can be monitored without fabricating electrodes, which allows resonators to be examined with minimal resist contamination.

B. Quality factor

An important metric for the performance of any nanoelectromechanical resonator is its quality factor, defined as

$$Q = 2\pi \frac{E_{\text{total}}}{\Delta E_{\text{cycle}}} = \frac{f}{\Delta f}, \quad (1)$$

where f is the resonant frequency of the resonator, Δf is the full width half power maximum of the Lorentzian amplitude response peak, E_{total} is the total energy stored in the resonator, and ΔE_{cycle} is the energy lost per cycle. Quality factor can be thought of as the purity of the tone with which a resonator vibrates: the higher the quality factor, the narrower the resonance peak in frequency space. High quality factors are desirable to optimize the performance of a nanomechanical resonator acting as a sensor or signal processor.

A commonly observed trend in NEMS is that as resonators are made smaller, quality factor tends to drop in inverse proportion to surface area to volume ratio R , presumably because surface effects begin to dominate the quality factor at small volumes. For example, single crystal silicon resonators of a variety of different shapes and sizes rarely exceed $RQ \sim 1000 \text{ nm}^{-1}$ because thinner resonators generally have lower quality factors.⁶⁸ It might be expected, therefore, that graphene's large surface area to volume ratio would cause it to have a low quality factor. The room temperature quality factors of the first graphene resonators, which were produced by mechanical exfoliation, seemed to be in keeping with this trend, with measured $Q \sim 80$,⁴⁴ $Q \sim 125$,⁴⁹ and $Q \sim 300$ (Ref. 69) ($RQ < 2000 \text{ nm}^{-1}$ assuming a thickness of 335 nm). Doubly clamped beams made from CVD graphene demonstrated similar quality factors ($Q < 250$).⁵⁹ Thicker variants of graphene, including graphene oxide⁵⁶ ($Q \sim 4000$) and epitaxial graphene⁵⁴ ($Q \sim 1000$) demonstrated higher Q , but not higher RQ products.

Recently, the achievement of quality factors as high as 2400 in CVD graphene drumhead resonators demonstrated that graphene could have RQ products exceeding 14000

nm^{-1} at room temperature, a value surpassed only by much larger high stress silicon nitride membrane resonators.⁶¹ This evidence suggests that despite its large surface area to volume ratio, graphene can have respectable quality factors. Since it has been theoretically predicted that clamping graphene membranes on all sides should improve the quality factor by eliminating “spurious edge modes,”⁷⁰ it was hypothesized that the clamping geometry of these resonators was important to their high quality factors. At lower temperatures, the quality factor of graphene resonators improves considerably, and values as high as $Q \sim 100000$ at 90 mK have been observed.⁷¹

The cause of the dissipation in graphene resonators is still unknown; however, it does show distinct characteristics (see Fig. 4). Studies of doubly clamped beam resonators made from both exfoliated^{49,69} and CVD (Ref. 59) graphene show similar dissipation as a function of temperature, with dissipation rapidly decreasing from 300 to 50–100 K, then decreasing more slowly, with $Q^{-1} \sim T^{0.3-0.4}$, at lower temperatures. This behavior bears a striking resemblance to that of carbon nanotube resonators at low temperature.⁷² Arrays of CVD graphene resonators have also enabled studies of dissipation as a function of size. In circular drumhead resonators made of graphene, quality factor was found to be linearly dependent on diameter, reaching $Q \sim 2400$ for resonators 22.5 μm in diameter.⁶¹ The physical reasons for the dependence of dissipation on temperature and size remain unknown, although theories^{73,74} have been proposed. Recent evidence suggests that nonlinear damping determines the resonant quality factor of both nanotube and graphene resonators at low temperatures and should be considered in any theory of dissipation in these ultrathin structures.⁷¹

C. Frequency reproducibility and tuning

One of the important landmarks in the application of graphene resonators will be the ability to produce a resonator of a given target frequency many times over. Mechanical exfoliation has performed poorly in this regard, because it is difficult to produce large numbers of devices, and also because

mechanically exfoliated graphene sheets are deposited with uncontrolled shape and tension, leading to unexpected fundamental modes of vibration.⁷⁵ Ripples are also an intrinsic feature of suspended graphene sheets that, if not controlled, could lead to a large variation in frequency from device to device.⁷⁶

New fabrication approaches have improved this reproducibility, although similar problems were observed in early epitaxial and CVD graphene devices. Arrays of resonators made from epitaxial graphene on silicon carbide were simple to produce in large numbers, but they showed wide variability in their resonance frequencies for a given length.⁵⁴ This variation was attributed to uncontrolled buckling in the membranes caused by compressive stress. Doubly clamped CVD graphene beams under tension also had wide variations in their frequencies and displayed complicated spectra with modes that were challenging to predict.⁵⁹ In the same experiment, however, it was found that the modes were more predictable for resonators that were clamped on all edges. Data taken for circular drumhead resonators in Ref. 61 supported this assertion. The current data suggest that resonators with free edges have more degrees of freedom, making it more difficult to control tension and rule out modes for which the edges are vibrating. Clamping the membrane on all sides alleviates these problems, and perhaps in addition increases quality factor as discussed earlier.

Because of graphene’s remarkable thinness and flexibility, its frequency can be adjusted over a wide range by applying electrostatic tension via a backgate. See Fig. 5 for the resonant frequency of one graphene resonator as a function of gate voltage. The strong dependence of frequency on gate voltage is promising for signal processing applications requiring a tunable frequency source. For example, graphene resonators could be useful as tunable filters for wireless communication applications.⁷⁷

D. Performance as sensors

One of the most exciting potential applications of graphene NEMS is sensing of mass,⁷⁸ force,⁷⁹ and position.⁸⁰

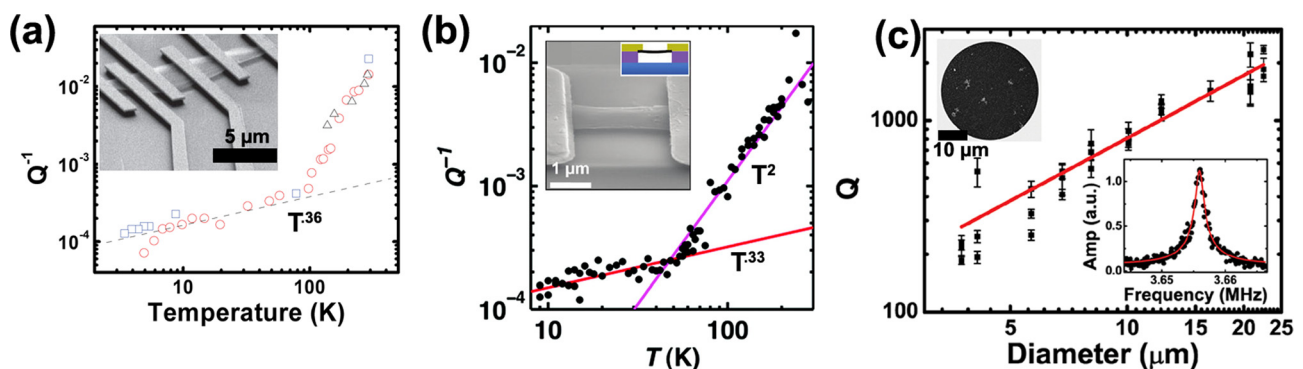


FIG. 4. (Color online) Properties of the quality factor of monolayer graphene. Doubly clamped exfoliated graphene resonators (Ref. 49) (a) and a doubly clamped CVD graphene resonator (Ref. 59) (b) display similar temperature dependence of quality factor. (c) Drumhead resonators (inset top left) made of monolayer CVD graphene display size-dependent quality factors at room temperature. Inset bottom right, the highest published quality factor for a monolayer graphene resonator at room temperature, $Q = 2400 \pm 300$. Reproduced from Ref. 61.

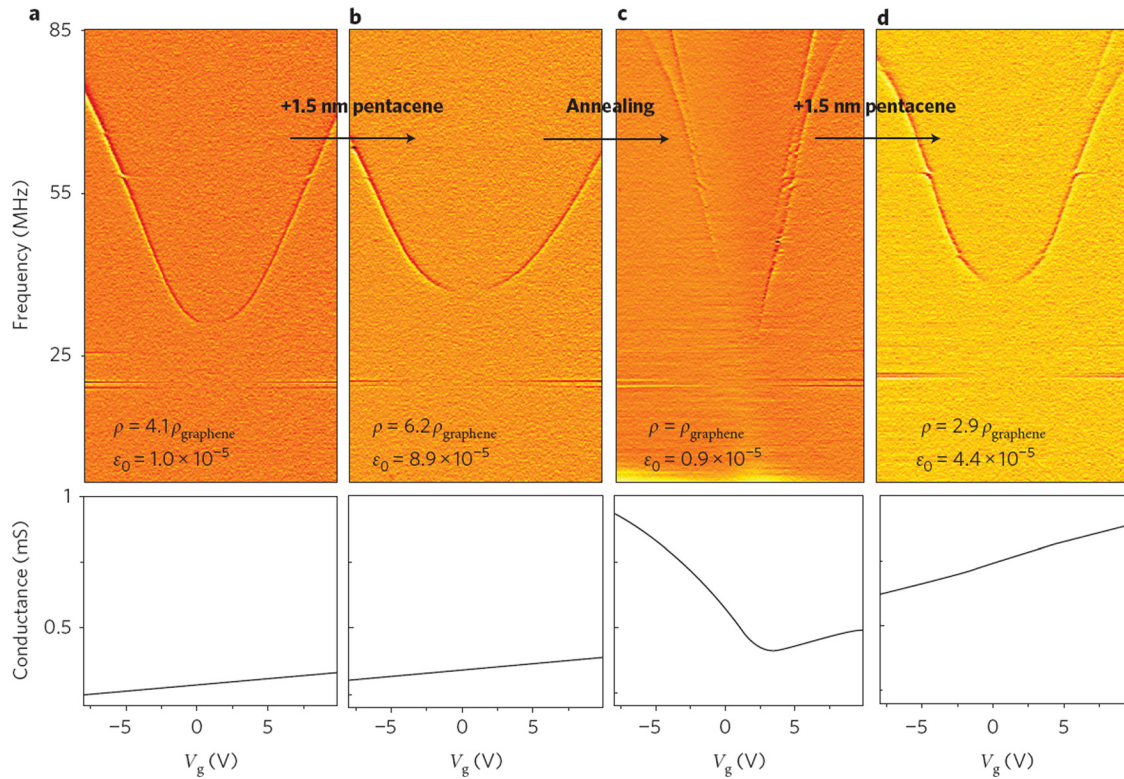


FIG. 5. (Color online) Electrically contacted graphene resonators can sense mass, tension, and charge simultaneously. In a color plot of dI/df as a function of frequency f and gate voltage, the graphene resonance stands out as a U-shaped feature. The dependence of the resonant frequency on gate voltage can be fit to extract the density ρ and strain ε_0 of the graphene sheet. Here, the deposition of pentacene on an as-fabricated exfoliated graphene resonator (a) causes the measured density and tension to increase (b). (c) Subsequent cleaning restores the density of the sheet to that of a pristine graphene resonator. (d) The addition of more pentacene increases the mass and the stress in the graphene. For each step, the charge can be studied by looking at the plots of conductance vs gate voltage. Figure adopted from Ref. 49.

Graphene's advantage as a sensor is that its low mass and flexibility make it couple strongly to the outside world. For example, the minimum mass resolvable with a mass sensor against a background of white noise is⁶²

$$\Delta m_{\min} = 2(m_{\text{eff}}/Q)10^{-\text{DR}/20}, \quad (2)$$

where m_{eff} is the effective mass of the resonator, Q is the quality factor, and DR is the dynamic range in decibels. Therefore, graphene's small mass gives it an impressive sensitivity. In one experiment,⁴⁹ a graphene resonator manufactured via mechanical exfoliation was estimated to have mass sensitivity ~ 2 zg with a detection bandwidth of ~ 3 Hz. As a two-dimensional material, graphene tends to have greater mass than its one-dimensional carbon nanotube counterparts, and better mass sensitivities have already been achieved at room temperature with carbon nanotubes.⁸¹ Significantly reducing at least one graphene dimension by, for example, fabricating resonators from graphene nanoribbons will be necessary for graphene to compete with carbon nanotubes in total resolvable mass. However, graphene has the advantage of a large surface area for mass flux capture, so that it is expected to have impressive sensitivity to mass per unit area. Experiments suggest that a circular drumhead resonator made of graphene should be able to resolve 3 pg cm^{-2} at room temperature, which is superior to the performance of quartz crystal microbalances.⁶¹

Another application at which graphene is expected to excel is force sensing.⁶¹ The minimum force/ $\sqrt{\text{Hz}}$ resolvable by a resonant sensor is

$$dF^f = (4k_{\text{eff}}k_B T / \omega Q)^{1/2}, \quad (3)$$

where k_{eff} is the effective spring constant, k_B is the Boltzmann constant, T is temperature, and ω is frequency. At room temperature, graphene resonators have achieved an estimated $dF^f \sim 200 \text{ aN/Hz}^{1/2}$.⁶¹ This number should be compared to the force sensitivity of ultrasensitive cantilevers used to do magnetic resonance imaging, which is $\sim 1 \text{ aN/Hz}^{1/2}$ at 100 mK.⁷⁹

Because graphene is both electrically and mechanically active, it can be used to simultaneously sense mass, stress, and charge. The data from one such experiment on an exfoliated graphene resonator is presented in Fig. 5. Before and after deposition of the analyte pentacene, the resonant frequency is plotted as a function of gate voltage V_g , which allows determination of the mass and stress by fitting the curve to the function:

$$f(V_g) = \frac{1}{2L} \sqrt{\frac{T_0 + T_e(V_g)}{\rho w}}, \quad (4)$$

where L , w , and ρ are the length, width, and density of the resonator, T_0 is the inherent tension in the device, and T_e is

the tension induced by the gate voltage.⁴⁹ Simultaneously, the conductance as a function of gate voltage is measured. When 1.5 nm pentacene is evaporated on an exfoliated graphene transistor, the mass of the device goes up, the stress increases, and the charge neutrality point moves to the right. After cleaning via Ohmic heating, the charge neutrality point moves to near zero gate voltage, and the resonance becomes more tunable, consistent with the pentacene leaving the device. These measurements demonstrate that graphene can simultaneously sense mass, force, and charge, which has numerous applications; for example, the simultaneous sensing of mass and charge of an analyte would be analogous to mass spectrometry. In addition, a similar way of reading out stress was used for more fundamental studies of the thermal expansion of graphene.⁶⁹

E. Membranes

Despite its thinness, graphene is impermeable to gases.⁴⁸ In combination with its force sensitivity, this fact gives graphene unique capabilities as a pressure sensor. The geometry shown in Figs. 2(c) and 2(d), for example, is $\sim 1 \mu\text{m}^3$ encapsulated on one side by a graphene sheet. Because the resonance frequency of the graphene depends on the pressure differential between the two sides of the membrane, measuring the frequency as a function of pressure produces a minimum that indicates when the pressure inside the chamber is equal to the pressure outside the chamber [Fig. 6(a)]. Hence, the pressure in a very small encapsulated volume can be probed, which is expected to be useful for investigating chemical reactions and phase transitions or detecting photons.⁴⁸

In addition, encapsulated small volumes are expected to be useful for biological investigation. Graphene has already been used as an electron transparent, conductive support for studying viruses⁸² and elongated DNA (Ref. 83) with transmission electron microscopy, but its impermeability to gases can add to this functionality—it could act as a transparent membrane that separates a fluid from the vacuum required to generate an electron beam; thus enabling imaging of biomolecules through

a fluid. The same fabrication techniques that have been used to fabricate suspended graphene NEMS can be used to create these structures. For example, Fig. 6(b) shows a yeast cell being imaged by SEM through a suspended graphene membrane produced by mechanical exfoliation.

IV. OUTLOOK AND CONCLUSIONS

As uniquely thin nanomechanical systems, graphene NEMS have the potential to be applied in more useful and more novel ways than the above-mentioned proof-of-principle demonstrations. As functionalization of graphene sheets advances,⁸⁴ their sensitivity to mass and stress could be wielded to enable highly sensitive biological and chemical sensing.⁸⁵ Furthermore, graphene resonators may be able to sense mass in unique ways; for example, a graphene drum resonator with degenerate eigenmodes should be able to determine both the mass and the position of an adsorbed particle using only measurements in a narrow band of frequency near the fundamental mode.⁸⁶ Along very different lines, graphene's high force sensitivity has elicited suggestions that it be used in cavity optomechanics.⁸⁷

In addition, there is much physics that remains to be explored for graphene mechanics. In particular, the source of mechanical dissipation in graphene resonators is only now being studied. If it can be understood, then graphene could act as an ideal system in which to study dissipation, as defects in this 2D crystal should be easier to control than in bulk. In addition, graphene resonators may prove useful for studying a mechanical system in its ground state, a long-sought experimental platform that was achieved only recently.⁸⁸ Cooling a mechanical system to its ground state is a challenging feat that requires extremely low temperatures and the ability to detect zero point motion on the order of $x_{\text{zp}} = \sqrt{\hbar/2m\omega}$.⁸⁹ Therefore, graphene's advantage in this area stems again from its small mass and its demonstrated ability to transduce motion into an electrical signal.

We should also note that many other two-dimensional materials have been studied and will provide interesting

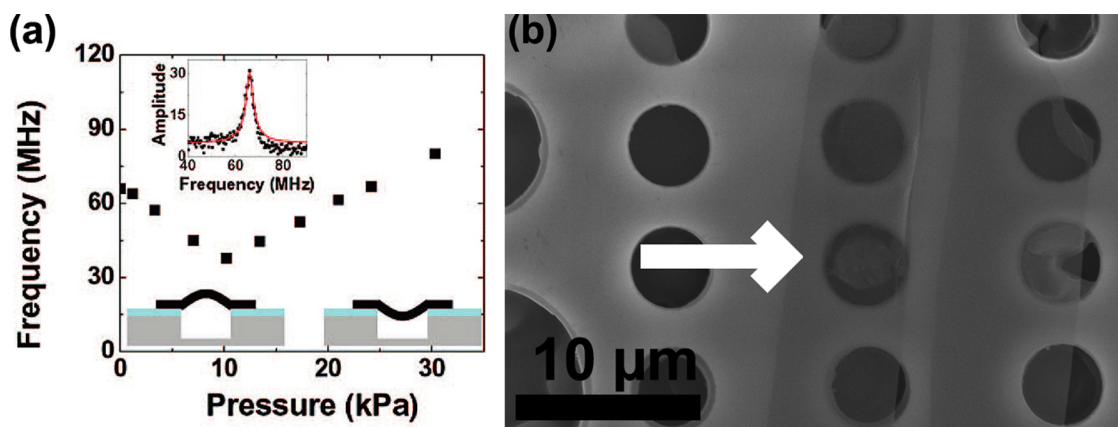


FIG. 6. (Color online) (a) Graphene is impermeable to gases, so that it can seal off a small volume of air. The pressure in a small volume enclosed by a graphene sheet can be measured by finding the resonance frequency of the graphene as a function of external pressure. Reproduced from Ref. 48. (b) A yeast cell is contained in a small volume of air beneath a graphene sheet. Because the graphene is transparent to electrons, it is possible to see the analyte inside the well, while the pressure inside the well can be determined via resonance measurements. (Barton *et al.*, unpublished work).

mechanical systems. Fluorinated graphene; for example, is transparent but also mechanically strong,^{90,91} so that it could be a good material from which to build high-finesse optomechanical cavities.⁹² Other two-dimensional systems of interest include h-BN, MoS₂, and NbSe₂, which are insulating, semiconducting, and metallic, respectively.^{24,93,94} In general, making mechanical devices out of single atomic layers opens up a wide range of possibilities enabled by the low mass and flexibility of these materials, while different materials will enable tailoring of the optical and electrical properties of the devices. As an example, thin NbSe₂ resonators have been used to study the physics of charge density waves at the nanoscale.⁹⁵

The field of nanomechanics has been pushing miniaturization for more than a decade, and with graphene and other 2D materials, it is finally reaching the limits of thinness. Graphene resonators have already proven that they can be manufactured in large arrays. They resonate with predictable frequencies, quality factors in the thousands at room temperature, and good dynamic range; they can also be applied to basic sensing of mass and force. Now, the challenge is to use this class of mechanical resonators to enable new applications and experiments.

ACKNOWLEDGMENTS

The authors thank A.M. van der Zande, I.R. Storch, and P. L. McEuen for useful discussions. The authors are grateful for support from the National Science Foundation through DMR-0908634 and through the Cornell Center for Materials Research, part of the NSF MRSEC Program.

- ¹A. K. Geim and K. S. Novoselov, *Nature Mater.* **6**, 183 (2007).
- ²A. K. Geim, *Science* **324**, 1530 (2009).
- ³K. I. Bolotin, K. J. Sikes, Z. Jiang, M. Klima, G. Fudenberg, J. Hone, P. Kim, and H. L. Stormer, *Solid State Commun.* **146**, 351 (2008).
- ⁴A. H. Castro Neto, F. Guinea, N. M. R. Peres, K. S. Novoselov, and A. K. Geim, *Rev. Mod. Phys.* **81**, 109 (2009).
- ⁵F. Schedin, A. K. Geim, S. V. Morozov, E. W. Hill, P. Blake, M. I. Katsnelson, and K. S. Novoselov, *Nature Mater.* **6**, 652 (2007).
- ⁶K. S. Kim, Y. Zhao, H. Jang, S. Y. Lee, J. M. Kim, J. H. Ahn, P. Kim, J. Y. Choi, and B. H. Hong, *Nature (London)* **457**, 706 (2009).
- ⁷Y. M. Lin, K. A. Jenkins, A. Valdes-Garcia, J. P. Small, D. B. Farmer, and P. Avouris, *Nano Lett.* **9**, 422 (2009).
- ⁸Y. M. Lin, C. Dimitrakopoulos, K. A. Jenkins, D. B. Farmer, H. Y. Chiu, A. Grill, and P. Avouris, *Science* **327**, 662 (2010).
- ⁹C. Lee, X. D. Wei, J. W. Kysar, and J. Hone, *Science* **321**, 385 (2008).
- ¹⁰K. M. Milaninia, M. A. Baldo, A. Reina, and J. Kong, *Appl. Phys. Lett.* **95**, 183105 (2009).
- ¹¹H. W. C. Postma, *Nano Lett.* **10**, 420 (2010).
- ¹²G. F. Schneider, S. W. Kowalczyk, V. E. Calado, G. Pandraud, H. W. Zandbergen, L. M. K. Vandersypen, and C. Dekker, *Nano Lett.* **10**, 3163 (2010).
- ¹³C. A. Merchant *et al.*, *Nano Lett.* **10**, 2915 (2010).
- ¹⁴S. Garaj, W. Hubbard, A. Reina, J. Kong, D. Branton, and J. A. Golovchenko, *Nature (London)* **467**, 190 (2010).
- ¹⁵J. C. Meyer, C. O. Girit, M. F. Crommie, and A. Zettl, *Nature (London)* **454**, 319 (2008).
- ¹⁶H. G. Craighead, *Science* **290**, 1532 (2000).
- ¹⁷K. L. Ekinci and M. L. Roukes, *Rev. Sci. Instrum.* **76**, 061101 (2005).
- ¹⁸X. K. Lu, H. Huang, N. Nemchuk, and R. S. Ruoff, *Appl. Phys. Lett.* **75**, 193 (1999).
- ¹⁹X. K. Lu, M. F. Yu, H. Huang, and R. S. Ruoff, *Nanotechnology* **10**, 269 (1999).
- ²⁰J. S. Bunch, Y. Yaish, M. Brink, K. Bolotin, and P. L. McEuen, *Nano Lett.* **5**, 287 (2005).
- ²¹Y. B. Zhang, J. P. Small, W. V. Pontius, and P. Kim, *Appl. Phys. Lett.* **86**, 073104 (2005).
- ²²Y. B. Zhang, J. P. Small, M. E. S. Amori, and P. Kim, *Phys. Rev. Lett.* **94**, 176803 (2005).
- ²³K. S. Novoselov, A. K. Geim, S. V. Morozov, D. Jiang, Y. Zhang, S. V. Dubonos, I. V. Grigorieva, and A. A. Firsov, *Science* **306**, 666 (2004).
- ²⁴K. S. Novoselov, D. Jiang, F. Schedin, T. J. Booth, V. V. Khotkevich, S. V. Morozov, and A. K. Geim, *Proc. Natl. Acad. Sci. U.S.A.* **102**, 10451 (2005).
- ²⁵P. Blake, E. W. Hill, A. H. C. Neto, K. S. Novoselov, D. Jiang, R. Yang, T. J. Booth, and A. K. Geim, *Appl. Phys. Lett.* **91**, 063124 (2007).
- ²⁶A. C. Ferrari *et al.*, *Phys. Rev. Lett.* **97**, 187401 (2006).
- ²⁷A. Gupta, G. Chen, P. Joshi, S. Tadigadapa, and P. C. Eklund, *Nano Lett.* **6**, 2667 (2006).
- ²⁸C. Berger *et al.*, *Science* **312**, 1191 (2006).
- ²⁹K. V. Emtsev *et al.*, *Nature Mater.* **8**, 203 (2009).
- ³⁰S. Stankovich, D. A. Dikin, G. H. B. Dommett, K. M. Kohlhaas, E. J. Zimney, E. A. Stach, R. D. Piner, S. T. Nguyen, and R. S. Ruoff, *Nature (London)* **442**, 282 (2006).
- ³¹D. A. Dikin, S. Stankovich, E. J. Zimney, R. D. Piner, G. H. B. Dommett, G. Evmenenko, S. T. Nguyen, and R. S. Ruoff, *Nature (London)* **448**, 457 (2007).
- ³²G. Eda, G. Fanchini, and M. Chhowalla, *Nat. Nanotechnol.* **3**, 270 (2008).
- ³³C. Gomez-Navarro, M. Burghard, and K. Kern, *Nano Lett.* **8**, 2045 (2008).
- ³⁴P. W. Sutter, J. I. Flege, and E. A. Sutter, *Nature Mater.* **7**, 406 (2008).
- ³⁵J. Coraux, A. T. N'Diaye, C. Busse, and T. Michely, *Nano Lett.* **8**, 565 (2008).
- ³⁶A. Reina, X. T. Jia, J. Ho, D. Nezich, H. B. Son, V. Bulovic, M. S. Dresselhaus, and J. Kong, *Nano Lett.* **9**, 30 (2009).
- ³⁷X. S. Li *et al.*, *Science* **324**, 1312 (2009).
- ³⁸S. Bae *et al.*, *Nat. Nanotechnol.* **5**, 574 (2010).
- ³⁹Z. Z. Sun, Z. Yan, J. Yao, E. Beitler, Y. Zhu, and J. M. Tour, *Nature (London)* **468**, 549 (2010).
- ⁴⁰P. Y. Huang *et al.*, *Nature (London)* **469**, 389 (2011).
- ⁴¹K. Kim, Z. Lee, W. Regan, C. Kisielowski, M. F. Crommie, and A. Zettl, *ACS Nano* **5**, 2142 (2011).
- ⁴²C. S. Ruiz-Vargas, H. L. Zhuang, P. Y. Huang, A. M. van der Zande, S. Garg, P. L. McEuen, D. A. Muller, R. G. Hennig, and J. Park, *Nano Lett.* **11**, 2259 (2011).
- ⁴³X. S. Li, C. W. Magnuson, A. Venugopal, R. M. Tromp, J. B. Hannon, E. M. Vogel, L. Colombo, and R. S. Ruoff, *J. Am. Chem. Soc.* **133**, 2816 (2011).
- ⁴⁴J. S. Bunch, A. M. van der Zande, S. S. Verbridge, I. W. Frank, D. M. Tanenbaum, J. M. Parpia, H. G. Craighead, and P. L. McEuen, *Science* **315**, 490 (2007).
- ⁴⁵J. C. Meyer, A. K. Geim, M. I. Katsnelson, K. S. Novoselov, T. J. Booth, and S. Roth, *Nature (London)* **446**, 60 (2007).
- ⁴⁶K. I. Bolotin, F. Ghahari, M. D. Shulman, H. L. Stormer, and P. Kim, *Nature (London)* **462**, 196 (2009).
- ⁴⁷X. Du, I. Skachko, F. Duerr, A. Luican, and E. Y. Andrei, *Nature (London)* **462**, 192 (2009).
- ⁴⁸J. S. Bunch, S. S. Verbridge, J. S. Alden, A. M. van der Zande, J. M. Parpia, H. G. Craighead, and P. L. McEuen, *Nano Lett.* **8**, 2458 (2008).
- ⁴⁹C. Y. Chen, S. Rosenblatt, K. I. Bolotin, W. Kalb, P. Kim, I. Kymissis, H. L. Stormer, T. F. Heinz, and J. Hone, *Nat. Nanotechnol.* **4**, 861 (2009).
- ⁵⁰Y. H. Xu, C. Y. Chen, V. V. Deshpande, F. A. DiRenno, A. Gondarenko, D. B. Heinz, S. M. Liu, P. Kim, and J. Hone, *Appl. Phys. Lett.* **97**, 243111 (2010).
- ⁵¹R. R. Nair, P. Blake, A. N. Grigorenko, K. S. Novoselov, T. J. Booth, T. Stauber, N. M. R. Peres, and A. K. Geim, *Science* **320**, 1308 (2008).
- ⁵²M. P. Levendorf, C. S. Ruiz-Vargas, S. Garg, and J. Park, *Nano Lett.* **9**, 4479 (2009).
- ⁵³B. Aleman *et al.*, *ACS Nano* **4**, 4762 (2010).
- ⁵⁴S. Shivaraman *et al.*, *Nano Lett.* **9**, 3100 (2009).
- ⁵⁵C. R. Dean *et al.*, *Nat. Nanotechnol.* **5**, 722 (2010).
- ⁵⁶J. T. Robinson, M. Zhaludtinov, J. W. Baldwin, E. S. Snow, Z. Q. Wei, P. Sheehan, and B. H. Houston, *Nano Lett.* **8**, 3441 (2008).
- ⁵⁷Y. Lee, S. Bae, H. Jang, S. Jang, S. E. Zhu, S. H. Sim, Y. I. Song, B. H. Hong, and J. H. Ahn, *Nano Lett.* **10**, 490 (2010).
- ⁵⁸X. S. Li, Y. W. Zhu, W. W. Cai, M. Borysiak, B. Y. Han, D. Chen, R. D. Piner, L. Colombo, and R. S. Ruoff, *Nano Lett.* **9**, 4359 (2009).

- ⁵⁹A. M. van der Zande *et al.*, *Nano Lett.* **10**, 4869 (2010).
- ⁶⁰L. Y. Jiao, B. Fan, X. J. Xian, Z. Y. Wu, J. Zhang, and Z. F. Liu, *J. Am. Chem. Soc.* **130**, 12612 (2008).
- ⁶¹R. A. Barton, B. Ilic, A. M. van der Zande, W. S. Whitney, P. L. McEuen, J. M. Parpia, and H. G. Craighead, *Nano Lett.* **11**, 1232 (2011).
- ⁶²K. L. Ekinci, X. M. H. Huang, and M. L. Roukes, *Appl. Phys. Lett.* **84**, 4469 (2004).
- ⁶³D. W. Carr and H. G. Craighead, *J. Vac. Sci. Technol. B* **15**, 2760 (1997).
- ⁶⁴V. Sazonova, Y. Yaish, H. Ustunel, D. Roundy, T. A. Arias, and P. L. McEuen, *Nature (London)* **431**, 284 (2004).
- ⁶⁵V. Gouttenoire, T. Barois, S. Perisanu, J. L. Leclercq, S. T. Purcell, P. Vincent, and A. Ayari, *Small* **6**, 1060 (2010).
- ⁶⁶T. Mashoff, M. Pratzner, V. Geringer, T. J. Echtermeyer, M. C. Lemme, M. Liebmann, and M. Morgenstern, *Nano Lett.* **10**, 461 (2010).
- ⁶⁷B. Ilic, S. Krylov, K. Aubin, R. Reichenbach, and H. G. Craighead, *Appl. Phys. Lett.* **86**, 193114 (2005).
- ⁶⁸X. Liu, J. F. Vignola, H. J. Simpson, B. R. Lemon, B. H. Houston, and D. M. Photiadis, *J. Appl. Phys.* **97**, 023524 (2005).
- ⁶⁹V. Singh, S. Sengupta, H. S. Solanki, R. Dhall, A. Allain, S. Dhara, P. Pant, and M. M. Deshmukh, *Nanotechnology* **21**, 165204 (2010).
- ⁷⁰S. Y. Kim and H. S. Park, *Nano Lett.* **9**, 969 (2009).
- ⁷¹A. Eichler, J. Moser, J. Chaste, M. Zdrojek, I. Wilson-Rae, and A. Bachtold, *Nat. Nanotechnol.* **6**, 339 (2011).
- ⁷²A. K. Huttel, G. A. Steele, B. Witkamp, M. Poot, L. P. Kouwenhoven, and H. S. J. van der Zant, *Nano Lett.* **9**, 2547 (2009).
- ⁷³C. Seoanez, F. Guinea, and A. H. Castro Neto, *Phys. Rev. B* **76**, 125427 (2007).
- ⁷⁴I. Wilson-Rae, R. A. Barton, S. S. Verbridge, D. R. Southworth, B. Ilic, H. G. Craighead, and J. M. Parpia, *Phys. Rev. Lett.* **106**, 047205 (2011).
- ⁷⁵D. Garcia-Sanchez, A. M. van der Zande, A. S. Paulo, B. Lassagne, P. L. McEuen, and A. Bachtold, *Nano Lett.* **8**, 1399 (2008).
- ⁷⁶W. Z. Bao, F. Miao, Z. Chen, H. Zhang, W. Y. Jang, C. Dames, and C. N. Lau, *Nat. Nanotechnol.* **4**, 562 (2009).
- ⁷⁷K. Jensen, J. Weldon, H. Garcia, and A. Zettl, *Nano Lett.* **7**, 3508 (2007).
- ⁷⁸B. Ilic, H. G. Craighead, S. Krylov, W. Senaratne, C. Ober, and P. Neuzil, *J. Appl. Phys.* **95**, 3694 (2004).
- ⁷⁹H. J. Mamin and D. Rugar, *Appl. Phys. Lett.* **79**, 3358 (2001).
- ⁸⁰M. D. LaHaye, O. Buu, B. Camarota, and K. C. Schwab, *Science* **304**, 74 (2004).
- ⁸¹K. Jensen, K. Kim, and A. Zettl, *Nat. Nanotechnol.* **3**, 533 (2008).
- ⁸²R. R. Nair *et al.*, *Appl. Phys. Lett.* **97**, 153102 (2010).
- ⁸³A. Cerf, T. Alava, R. A. Barton, and H. G. Craighead, "Transfer-printing of single DNA molecule arrays on graphene for high resolution electron imaging and analysis."
- ⁸⁴Y. Cui, S. N. Kim, S. E. Jones, L. L. Wissler, R. R. Naik, and M. C. McAlpine, *Nano Lett.* **10**, 4559 (2010).
- ⁸⁵P. S. Waggoner and H. G. Craighead, *Lab Chip* **7**, 1238 (2007).
- ⁸⁶J. Atalaya, J. M. Kinaret, and A. Isacsson, *EPL* **91**, 48001 (2010).
- ⁸⁷G. Anetsberger, O. Arcizet, Q. P. Unterreithmeier, R. Riviere, A. Schliesser, E. M. Weig, J. P. Kotthaus, and T. J. Kippenberg, *Nat. Phys.* **5**, 909 (2009).
- ⁸⁸A. D. O'Connell *et al.*, *Nature (London)* **464**, 697 (2010).
- ⁸⁹T. Rocheleau, T. Ndukum, C. Macklin, J. B. Hertzberg, A. A. Clerk, and K. C. Schwab, *Nature (London)* **463**, 72 (2010).
- ⁹⁰J. T. Robinson *et al.*, *Nano Lett.* **10**, 3001 (2010).
- ⁹¹R. R. Nair *et al.*, *Small* **6**, 2877 (2010).
- ⁹²J. C. Sankey, C. Yang, B. M. Zwickl, M. Jayich, and J. G. E. Harris, *Nat. Phys.* **6**, 707 (2010).
- ⁹³C. Lee, Q. Y. Li, W. Kalb, X. Z. Liu, H. Berger, R. W. Carpick, and J. Hone, *Science* **328**, 76 (2010).
- ⁹⁴B. Radisavljevic, A. Radenovic, J. Brivio, V. Giacometti, and A. Kis, *Nat. Nanotechnol.* **6**, 147 (2011).
- ⁹⁵S. Sengupta, H. S. Solanki, V. Singh, S. Dhara, and M. M. Deshmukh, *Phys. Rev. B* **82**, 155432 (2010).